Habitat complexity defines global biological and societal landscapes

James Cant[1,2*], Nina Schiettekatte[3], Elizabeth M. P. Madin[3], Joshua S. Madin[3] & Maria Dornelas[1,4]

1. Centre for Biological Diversity, University of St Andrews, St Andrews, Fife, KY16 9TH, UK.
2. Department of Biology, University of Oxford, South Parks Road, Oxford, OX1 3RB, UK.
3. Hawai'i Institute of Marine Biology, University of Hawai'i at Manoa, Kaneohe, HI 96744, USA.
4. MARE, Guia Marine Laboratory, University of Lisbon, Cascais, Portugal.

* Corresponding author: james.cant91@gmail.com

Author Contributions: JC, NS, EMPM, JSM, and MD all devised the initial research idea. MD, JSM, and EMPM sourced project funding. JC carried out all analyses with support from NS, JSM, and MD. JC led manuscript write up with all authors contributing to subsequent drafts.

Conflicts of Interest: The authors declare that there are no conflicts of interest associated with this piece of work.

Data Availability Statement: The global maps of geometric complexity presented in this manuscript have been archived and will be made publicly available once this manuscript has been accepted for publication. All the R scripts used in developing these maps and implementing all analyses discussed throughout this manuscript have been uploaded to GitHub (https://github.com/CantJ/Global-Geometric-Complexity), and will also be made publicly available following publication of this manuscript.

Summary

The three-dimensional structure of land- and seascapes sits at the boundary of biotic and abiotic geographies, linking geological processes to the configuration of localised weather patterns and oceanographic regimes and determines whether, and how, organisms access and use available resources[1–3]. Evaluating the relationship between habitat complexity and biodiversity has long been a prominent feature of ecological research[4,5]. However, inconsistencies in approaches used in defining and quantifying habitat complexity have so far precluded cross-system comparisons[6,7], preventing synthetic assessments into the ecological and evolutionary role of habitat complexity. Here we expand a framework developed for quantifying the structural complexity of coral reef environments[8] to present a scalable solution for estimating the complexity of terrestrial and aquatic habitats globally. We present high-resolution (1.87 × 1.87 km pixel size) maps detailing global patterns in the geometric complexity measures of height range, rugosity, and fractal dimension, and illustrate how key differences in these characteristics across marine and terrestrial landscapes serve to delineate the configuration of different biomes and anthromes. Overall, this work refines understanding for the mechanisms through which habitat complexity defines the global configuration of society and nature and offers a platform for exploring these interactions at varying spatial scales.

Main

The physical structure of natural environments sets the stage onto which ecological, geological, and climatic processes shape global biodiversity, human civilisation, and their interactions[7,9]. Indeed, whilst climatic regimes are a major determinant of global species richness trends[10], abiotic structure coordinates the spatio-temporal configuration of climate systems, thereby mediating climate exposure and resource availability and access[1,11]. Topographical and geological patterns also influence the taxonomic and functional diversity of forest ecosystems, subsequently underpinning their localised provision of biotic complexity and niche variety[5]. Moreover, the shape of natural habitats provides a wealth of green, blue and white spaces that support physical and mental wellbeing and agricultural diversification, thus supporting human health and socioeconomic development[9,12]. Understanding global patterns in habitat structure is key to safeguarding biodiversity, ensuring the sustainable use of natural resources, maintaining human livelihoods and public health, and for conserving earth's unique and diverse natural heritage[13–15].

Our growing appreciation for the role of structural habitat complexity (henceforth habitat complexity) in the development of natural and anthropogenic systems is accelerating calls for greater insight into the mechanisms interfacing abiotic and biotic systems[16–18]. Conservation initiatives, such as *Conserving Nature's Stage*, argue that the successful conservation of biodiversity relies upon protecting the enduring landscape features upon which it exists[19,20]. Access to the diversity of habitats necessary for maintaining genetic diversity is also considered amongst the legal Rights of Nature[21]. In light of continual land-use change, climatic change, and unmet conservation targets, the UN's sustainable development goals (SDG's) reflect the need for humanity's use of global resources to not undermine our biotic life-support system[22,23]. However, despite habitat complexity being a prominent feature of ecological research, the term itself is poorly defined, prompting a lack of consensus for how it

should be quantified and measured[6,24]. As a result, existing insight into the underlying role of habitat complexity in determining the configuration of natural systems is fragmented across isolated systems and often evaluated using incomparable approaches[2].

Here, we provide a comprehensive, quantitative assessment of global habitat complexity patterns using a geometric framework established for quantifying the structural complexity of coral reef environments[8]. Complementing recent efforts to classify global ecosystem types[11], we use this approach to demonstrate how ecosystems are aligned along a complexity gradient based on their relative geometric attributes, in turn offering insight into the link between the processes driving the formation of abiotic habitats and their subsequent association with distinct biological assemblages. We also illustrate mechanistic signals across the association between habitat geometry and socioeconomic drivers, highlighting the link between socio-economic development and global habitat structure. Consequently, this work represents a unified approach for evaluating the role of habitat complexity in (1) mediating the configuration of society and nature, (2) influencing the success of conservation efforts, and (3) can be used to monitor the success of ongoing sustainable development targets.

Assessing habitat complexity across ecosystems

Heterogeneity in habitat structure (*i.e.*, its complexity) is assumed to be important for maintaining biodiversity[25]. This assertion forms a key component of the theory of Island Biogeography, with more structurally complex environments thought to accommodate a greater diversity of available niche space and, therefore, support higher species richness[26,27]. However, this assumption is contradicted by the area-heterogeneity trade-off concept, which predicts that the greater niche variety brought about by enhanced habitat complexity, likely reduces realised niche space, thereby reducing population sizes and increasing the likelihood of local extirpation[28]. How these two ecological processes interact holds the key for evaluating

and forecasting localised patterns of biodiversity change in response to climate shifts, habitat fragmentation, and ecological restoration.

To assess global-scale patterns in habitat complexity we quantified the complexities of global land- and seascapes, using the geometric measures of, *height range* (ΔH), *rugosity,* (R) and *fractal dimension* (D; Fig. 1). To produce these global maps of structural habitat complexity, we applied a geometric framework originally established for quantifying coral reef structure[8], to a global elevation model sourced from the General Bathymetric Chart of the Oceans (GEBCO)[29]. As measures of geometric complexity, ΔH captures the variation between the maximum and minimum elevation of a surface, R describes the true surface area of the surface, and D details the shape filling capacity of a surface (increases in D correspond with an increase in the convolution of a surface)[30].

Global patterns in our measures of ΔH, R, and D, reveal key variation across the habitat complexity regimes of different marine and terrestrial environments. First, the greatest height range and highest rugosity environments are associated with the Himalayan, Andean, and Mid-Atlantic mountain ranges (Fig. 1b & c). Second, dense areas of higher fractal dimension are visible in the arctic tundras of North America and Siberia, the Amazonian and Patagonian regions of South America, and pockets of north central Africa (Fig 1a). Third, a clear difference emerges between the fractal nature of marine and terrestrial environments (Fig. 1a), with the marine landscape characterised by more extensive regions of low fractal dimension.

At a more local scale, isolating the relative fractal dimension and rugosity regimes of selected locations within the Amazonian Basin (AB; Fig. 2a), the Mariana Trench (MT; Fig. 2b), and the Sahara Desert (SD; Fig. 2c), demonstrates how habitat rugosities align with local elevation patterns. In comparison with the other locations, the Mariana Trench is characterised by a high density of more rugose environments (mean R: AB = 0.001, MT = 0.020, SD < 0.001). Meanwhile, the contours associated with the river channels spanning the Amazon River

basin are visible across its rugosity regime (Fig 2a). However, unlike estimates of rugosity, the fractal dimension of surface habitats does not conform with their more obvious structural features, offering a very different perspective of natural landscapes. When viewed through the lens of its fractal dimension, the main channel of the Mariana Trench almost disappears (Fig. 2b). Alternatively, the Sahara Desert and the Amazon river basin, are characterised by regions of higher fractal dimension, corresponding with their less rugged terrains (Fig. 2). Higher fractal dimension is often associated with an increase in niche diversity, and therefore species richness[31–33]. Perhaps it is not surprising then, that the Amazonian Basin, considered amongst the most biodiverse ecosystems, is underpinned by dense regions of higher fractal dimension (mean D: AB = 2.29, MT = 2.15, SD = 2.22). However, that the Sahara Desert, a comparatively more inhospitable environment, also maintains regions of higher fractal dimension, emphasises that it is the interaction between each of an ecosystem's individual attributes of structural complexity and their local climate regime that defines their associated biodiversity[1].

The mechanistic drivers of a global complexity gradient

The relative rugosity and fractal dimension characteristics of natural environments positions ecosystems along a gradient of habitat complexity (Fig. 3) and can be used to explore the mechanisms through which environmental structures mediate biodiversity and socio-economic development (Fig. 4). Recently, the IUCN established a function-based ecosystem typology classification (FET) aimed at supporting the development of ecosystem management and restoration initiatives while enhancing our ability to predict the response of ecosystem functioning to ongoing global change[11]. These ecosystem classes align along a gradient defined by their rugosity and fractal dimension characteristics (Fig. 3a; r^2 = 0.172 [95% CI: 0.058, 0.292]), highlighting the role played by the geometric complexity of environments in delineating abiotic and biotic regimes to underpin the diversity of earth's natural heritage. Aside

158 from the clear distinction between the complexities of marine and terrestrial ecosystem types,
159 this gradient reveals how, across all realms, ecosystems of similar classifications maintain
160 comparable complexity regimes (*i.e.*, wetland environments are all characterised by higher
161 fractal dimension and low rugosities; Fig. 3a). This pattern does not mean that habitat
162 complexity is the driving force underpinning global biodiversity patterns. However, it again
163 emphasises how by interacting with local climate factors, the geometric structure of natural
164 environments can preserve and perpetuate the spatial distributions of particular ecosystem
165 states. For instance, despite possessing similar ratios of rugosity and fractal dimension, oceanic
166 temperate rainforests and polar alpine cliff ecosystems support different biological
167 communities due to their differing climate exposures. Yet, during the mid-Cretaceous (92 to
168 83 million years ago), under a far warmer global climate, the habitat structure associated with
169 contemporary polar alpine cliff ecosystems supported diverse oceanic temperate rainforests[34].

170 Habitat morphology and topography influence whether, how, and when, organisms can
171 access available resources[3]. The FET framework includes the presence of geomorphic features
172 (the categorisation of topographic reliefs and slope aspects as visible structural features[35]) as a
173 classification criteria[11]. With our measures of height range, rugosity and fractal dimension
174 extracted from topographical records, it is not surprising that ecosystem types fall along a
175 complexity gradient. However, the FET framework includes geomorphic indices as indirect
176 modulators of resource access[11]. Here, the alignment of ecosystem types along a complexity
177 gradient attests to a much more direct association between the structural composition of natural
178 habitats and the configuration of global biodiversity.

179 The importance of evaluating the direct association between habitat complexity and
180 biological assembly has given rise to novel ecological concepts such as *geodiversity*[14]. Akin to
181 an abiotic analogue of the term biodiversity, geodiversity combines measures of the richness
182 of structural features and processes comprising different environments[36]. Geodiversity offers a

183 measure of niche diversity that has been illustrated to support the maintenance of ecosystem
184 function and functional diversity[18]. However, assessments of geodiversity overlook how the
185 structural elements that comprise different environments subsequently shape those
186 environments[37]. Indeed, measures of geometric structure offer a differing perspective regarding
187 the heterogeneity regimes imposed by different environments, compared to geodiversity (Fig.
188 4a). While rugosity, height range and geodiversity explain similar trends in the structural
189 heterogeneity of natural environments (r^2: ΔH = 0.3619 [0.3603, 0.3634], R = 0.3766 [0.3751,
190 0.3782]), patterns in fractal dimension and geodiversity are unrelated across the terrestrial
191 landscape (r^2 = 0.0978 [0.0964, 0.0992]). Measures of fractal dimension and geodiversity can
192 therefore offer independent perspectives into how the structural complexity of natural
193 ecosystems mediates the configuration of global biodiversity; emphasising the importance of
194 including various measures of structural heterogeneity within assessments aimed at informing
195 conservation action and ecosystem management[38].

196 The complexity of landscapes also has profound impacts on multiple aspects of human
197 society (*e.g.*, tourism, agriculture, mobility, and wellbeing)[9,12]. Patterns across the structural
198 complexities of natural habitats reveals insight into how geometric structure influences the way
199 human society uses natural environments, but also into how this usage impacts upon the
200 underlying structure of those environments (Fig 3b). The arrangement of global land-use types
201 based on their rugosity and fractal dimension aligns somewhat with the same gradient observed
202 across the complexities of different ecosystem types. However, land-use types corresponding
203 with increased human modification (*i.e.*, urban and cropland environments) display reduced
204 complexities (R and D) when compared to more 'natural' land-use types (Fig. 3b). This pattern
205 may arise from human activity diminishing the complexity of natural environments and/ or by
206 humans selecting less complex environments for development[12,24]. Whilst we are unable to

distinguish between cause and effect with static layers, both instances are likely true across the global landscape.

A similar cyclical relationship between human society and habitat complexity is evident across the associations between our measures of ΔH, R, and D, and global human population density (Fig. 4b). With mountain ranges and high alpine regions (areas associated with high estimates of ΔH and R) typically associated with a reduction in the space and arable land needed for agriculture and food production, the development of human settlements has often gravitated towards flatter, more lowland environments[39]. Accordingly, human population densities are negatively correlated with our global measures of height range and rugosity (Fig 4b; r^2: ΔH = 0.1738 [0.1725, 0.1750], R = 0.1741 [0.1729, 0.1754]). Intriguingly, human population densities are also negatively associated with fractal dimension (Fig. 4b; r^2 = 0.1754 [0.1741, 0.1767]). The surface descriptors of height range, rugosity, and fractal dimension are constrained in such a way that it is extremely rare for natural surfaces to exhibit low estimates of all three measures[8]. Thus, human population densities being associated with environments that exhibit low ΔH, R, and D may be indicative that anthropogenic activity simplifies the geometric, compositional, and configurational structure of natural landscapes[40–42].

Future research

Our global-scale assessment of geometric habitat structure emphasises the role of habitat complexity in mediating the configuration of natural and anthropogenic communities. Having long appreciated the association between diversity and area, a recent focus of ecological research has been devoted to quantifying the mechanistic drivers linking biodiversity and area. Naturally, it is not changes in area *per-se* that determine trends in species richness but the changes in environmental structure it entails. Colonisation, extinction, and speciation are fundamental drivers of species richness patterns[43], and are acutely linked to the structural shape of the landscape[3]. Through the shaping of dispersal pathways and niche partitioning, prehistoric

shifts in landscape topography have defined the contemporary arrangement of global biodiversity more so than prevailing climatic regimes[44]. Thus, forecasting how natural communities will respond to ongoing global change requires the evaluation of the intrinsic association between biodiversity and abiotic habitat structure. Moreover, nature does not exist in pristine isolation, with the majority of global ecosystems facing some form of direct anthropogenic pressure[45–47]. How we interact with and utilse our local environment is also mediated by patterns in habitat complexity. So too is how these natural environments respond to exploitation. We have demonstrated how the same geometric theory offers informative and relevant insights into the mechanisms through which habitat structure underpins the configuration of global biomes and anthromes. Having illustrated the applicability of our approach at the global-scale, the methodology through which we scaled-up the geometric assessment of surface habitats is sufficiently flexible for accommodating assessments of habitat complexity at varying resolutions across local, regional, and continental terrains. Thus our approach here opens up avenues for addressing how the distribution of topographical boundaries and microhabitats configures the nuanced processes of speciation, diversification, isolation, and connectivity[31,33], and how these processes will interact with anthropogenic pressures and ongoing global change.

Methods

Briefly, our study comprised the following sequence of steps: generating global maps of selected complexity indices; evaluating ecosystem and land-use associated complexity characteristics; and quantifying the association between habitat complexity and additional abiotic and biotic mechanisms. All spatial analyses were carried out using R[48] and QGIS[49].

Generating global complexity maps

We estimated global patterns in height range (ΔH), rugosity (R), and fractal dimension (D) using the GEBCO 2023 global ocean and land terrain model (including ice surface elevation)[29]. Initially merging the corresponding raster tiles downloaded from GEBCO (https://www.gebco.net/) to produce a 15 arc-second resolution (EPSG: 4326, WGS84) global map of surface elevation in metres, we reprojected this elevation model (henceforth digital elevation model [DEM]) to an equal-area Mollweide projection (EPSG: 54009) at a resolution of 187 m (L_0). From this DEM, using the associated functions contained in the *habtools* package[50] we then extracted estimates of ΔH, R, and D, at a scale of 1870 m (L; one order of magnitude greater than L_0). Briefly, this extraction involved separating our DEM file into longitudinal tiles each corresponding with a longitudinal distance equal to L (equivalent to 10 pixel columns). Using multicore processing, implemented using the *foreach* and *doParallel* packages[51,52], we iteratively processed each longitudinal tile to extract estimates of ΔH (the difference between the maximum and minimum elevation of a surface), R (the surface area of a surface), and D (calculated using the associations between ΔH, R, and D in the geometric plane equation from Torres-Pulliza *et al.*[8] [equation 1]) for each latitudinal band (each band corresponded with 10 rows, equivalent to a distance of L, resulting in a series of $L \times L$ pixels):

$$D = 3 - \frac{\log\left(\frac{\Delta H}{\sqrt{2}L_0\sqrt{R^2-1}}\right)}{\log\left(\frac{L}{L_0}\right)} \quad (1)$$

Next, we carried out data cleaning, omitting all estimates that, (1) violated geometric theory for surface habitats ($\Delta H < 0$; $R < 1$; $2 > D > 3$; 85,183 entries, 0.046% of initial sample) and, (2) corresponded with non-fractal (flat) pixel cells ($\Delta H = 0$, $R = 1$ & $D = 2$; 435,225 entries, 0.233% of initial sample). We omitted non-fractal cells on the basis that, at a scale of 1870m, perfectly flat landscapes do not exist and instead represent artefacts present in the original elevation model[53], or accuracy errors introduced during model reprojection. Prior to collating our estimates for each complexity measure into separate spatial raster files we transformed all

ΔH and R estimates according to their expression in the geometric plane equation[8], such that rugosity is expressed as $R^2 - 1$ and height range is expressed as $\frac{\Delta H}{\sqrt{2}L_0}$.

Comparing ecosystem and land use type complexities

We evaluated patterns across our estimates of R and D associated with differing ecosystem and land use classifications. Carrying out this assessment involved assigning each pixel across our complexity maps to particular ecosystem and land-use types. Firstly, we used the IUCN ecosystem typology classification framework[11] to define our ecosystem types and their spatial distributions across the global landscape[54] (all distribution maps were reprojected to a Mollweide projection). Next we quantified spatial patterns in land-use categories using a satellite derived global land cover map sourced from the Copernicus Climate Change Service (C3S)[55]. From the C3S data portal, we sourced an .nc file comprising different global land cover variables derived from satellite surveys carried out during 2022. From this file we extracted the associated land cover class layer using the *raster* package[56], which we then reprojected to a Mollweide projection (EPSG: 54009) at a resolution of 1870m (L), all whilst ensuring the finalised map extent corresponded with that of our DEM. For the assessment of both ecosystem and land-use associated complexities we overlayed the corresponding spatial files detailing the spatial distributions of selected ecosystem and land use types (Tables S1 & S2) onto our global complexity maps to isolate the values of R and D associated with each ecosystem and land use category. Using the *brms* package[57], we performed polynomial Bayesian regression to evaluate the relationship between mean R and D estimates across ecosystem types. We opted for this non-linear format following 'leave-one-out' cross-validation model comparisons between non-linear and linear formats. For this analysis we implemented a single model consisting of 20 Markov Chains, each comprising 5000 iterations (including 1000 warm-up iterations).

Evaluating associated mechanisms

Focusing on the terrestrial landscape, we evaluated how our estimates of ΔH, R, and D correspond with two established drivers of global biotic and abiotic regimes: geodiversity (G), and human population density (PD). We sourced geodiversity estimates from a global map of terrestrial geodiversity developed during an assessment of geodiversity representation across UNESCO geoparks[58] (EPSG: 54009). Originally, sourced at a resolution of 250m, this global map was reprojected to a resolution of 1870m (L) and to an extent equal to that of our global complexity rasters. Meanwhile, we obtained global data on human population densities from the Gridded Population of the World[59]. We downloaded a map of the global population density recorded in 2020 at a 30 arc-second resolution (EPSG: 4326) which we subsequently reprojected to a 1870m resolution in a Mollweide projection. Aligning corresponding pixel values across these spatial maps, then allowed for extracting corresponding estimates for ΔH, R, D, G, and PD, from which we retained the pixel cells with complete entries for all variables (~38 million pixels). Following data omission, we used the *terra* package[61] to test each of our geometric complexity variables (ΔH, R, and D) for spatial autocorrelation, by computing Moran's I statistic for each measure (I: $\Delta H = 0.883$; $R = 0.805$; $D = 0.476$, assuming a Queen's case nearest neighbour matrix, *i.e.*, all adjacent cells including diagonals). Lastly, we transformed our population density variable for normality. This transformation took the form of a power transformation ($y^{0.05}$) applied only to non-zero entries.

We analysed the pairwise relationships between each of our geometric variables (ΔH, R and D) and G, using generalised additive models (GAMs) and Monte-Carlo resampling. To assess each pairwise relationship we implemented our GAMs using the *mgcv* package[60], repeating each pairwise comparison 1000 times on a randomly selected sub-sample of 1000 data points (0.0026% sample), each time computing the associated model's r^2 value and predicted relationship. We fitted all models to a gaussian distribution, with geodiversity set as

the predictor variable, and with a fixed spatial smoothing term included (defined by the covariates of latitude and longitude) to account for the spatial autocorrelation evident across our complexity variables. ($I > 0$).

Also implemented using Monte-Carlo resampling, we analysed the pairwise relationships between each of our geometric variables and *PD*, using hurdle models implemented via a Bayesian framework in *brms*. Using this hurdle approach allowed us to separately model the probability of zero population density as a function of geometric complexity, and the relationship between non-zero population densities and geometric complexity. We repeated each pairwise hurdle model 1000 times on a randomly selected sub-sample of 1000 data points, each time retaining the model's r^2 value, predicted non-zero relationship, and its hurdle coefficients (probability of being zero). We modelled the relationship between complexity and non-zero population density using a gamma distribution, and again, included a fixed spatial smoothing term to account for spatial autocorrelation across our complexity variables.

Acknowledgements

This research was supported by a joint NSF-NERC grant (Award number: 1948946) to MD, JM and EMPM.

References

1. Coelho, M. T. P. *et al.* The geography of climate and the global patterns of species diversity. *Nature* **622**, 537–544 (2023).
2. Kovalenko, K. E., Thomaz, S. M. & Warfe, D. M. Habitat complexity: Approaches and future directions. *Hydrobiologia* **685**, 1–17 (2012).
3. Badgley, C. *et al.* Biodiversity and Topographic Complexity: Modern and Geohistorical Perspectives. *Trends Ecol. Evol.* **32**, 211–226 (2017).

4. MacArthur, R. H. & MacArthur, J. W. On Bird Species Diversity. *Ecology* **42**, 594–598 (1961).

5. Ehbrecht, M. *et al.* Global patterns and climatic controls of forest structural complexity. *Nat. Commun.* **12**, 519 (2021).

6. Loke, L. H. L. & Chisholm, R. A. Measuring habitat complexity and spatial heterogeneity in ecology. *Ecol. Lett.* **25**, 2269–2288 (2022).

7. Madin, J. S. *et al.* A word on habitat complexity. *Ecol. Lett.* **26**, 1021–1024 (2023).

8. Torres-Pulliza, D. *et al.* A geometric basis for surface habitat complexity and biodiversity. *Nat. Ecol. Evol.* **4**, 1495–1501 (2020).

9. Alahuhta, J. *et al.* Acknowledging geodiversity in safeguarding biodiversity and human health. *Lancet Planet Health* **6**, 987–92 (2022).

10. Pecl, G., Araujo, M. B., Bell, J. D., Blanchard, J. & Bonebrake, T. C. Biodiversity redistribution under climate change: Impacts on ecosystems and human well-being Publication Details. *Science* **355**, 1–9 (2017).

11. Keith, D. A. *et al.* A function-based typology for Earth's ecosystems. *Nature* **610**, 513–518 (2022).

12. Nelson, K. S. & Burchfield, E. K. Landscape complexity and US crop production. *Nat. Food* **2**, 330–338 (2021).

13. Schrodt, F. *et al.* To advance sustainable stewardship, we must document not only biodiversity but geodiversity. *PNAS* **116**, 16155–16158 (2019).

14. Schrodt, F. *et al.* The status and future of essential geodiversity variables. *Philos. Trans. R. Soc. A* **382**, 1–18 (2024).

15. Knudson, C., Kay, K. & Fisher, S. Appraising geodiversity and cultural diversity approaches to building resilience through conservation. *Nat. Clim. Change* **8**, 678–685 (2018).

16. Zarnetske, P. L. *et al.* Towards connecting biodiversity and geodiversity across scales with satellite remote sensing. *Glob. Ecol. Biogeogr.* **28**, 548–556 (2019).

17. Zarnetske, P. L. *et al.* The Interplay Between Landscape Structure and Biotic Interactions. *Curr. Landsc. Ecol. Rep.* **2**, 12–29 (2017).

18. Vernham, G. *et al.* Understanding trait diversity: the role of geodiversity. *Trends Ecol. Evol.* (2023) doi:10.1016/j.tree.2023.02.010.

19. Beier, P., Hunter, M. L. & Anderson, M. Special Section: Conserving Nature's Stage. *Conserv. Biol.* **29**, 613–617 (2015).

20. Lawler, J. J. *et al.* The theory behind, and the challenges of, conserving nature's stage in a time of rapid change. *Conserv. Biol.* **29**, 618–629 (2015).

21. Epstein, Y., Ellison, A. M., Echeverría, H. & Abbott, J. K. Science and the legal rights of nature. *Science* **380**, eadf4155 (2023).

22. Steffen, W. *et al.* Planetary boundaries: Guiding human development on a changing planet. *Science* **347**, 1259855 (2015).

23. Reyers, B. & Selig, E. R. Global targets that reveal the social–ecological interdependencies of sustainable development. *Nat. Ecol. Evol.* **4**, 1011–1019 (2020).

24. Green, D. G., Klomp, N., Rimmington, G. & Sadedin, S. *Complexity in Landscape Ecology*. vol. 4 (Springer, The Netherlands, 2006).

25. Tews, J. *et al.* Animal species diversity driven by habitat heterogeneity/diversity: The importance of keystone structures. *J. Biogeogr.* **31**, 79–92 (2004).

26. MacArthur, R. H. & Wilson, E. O. *The Theory of Island Biogeography*. (Princeton University Press, 1967).

27. Stein, A., Gerstner, K. & Kreft, H. Environmental heterogeneity as a universal driver of species richness across taxa, biomes and spatial scales. *Ecol. Lett.* **17**, 866–880 (2014).

28. Allouche, O., Kalyuzhny, M., Moreno-Rueda, G., Pizarro, M. & Kadmon, R. Area–heterogeneity tradeoff and the diversity of ecological communities. *Proc. Natl. Acad. Sci.* **109**, 17495–17500 (2012).

29. GEBCO Compilation Group. GEBCO 2023 Grid. (2023).

30. Warfe, D. M., Barmuta, L. A. & Wotherspoon, S. Quantifying Habitat Structure: Surface Convolution and Living Space for Species in Complex Environments. *Oikos* **117**, 1764–1773 (2008).

31. Johnson, M. P., Frost, N. J., Mosley, M. W. J., Roberts, M. F. & Hawkins, S. J. The area-independent effects of habitat complexity on biodiversity vary between regions. *Ecol. Lett.* **6**, 126–132 (2003).

32. Gámez, S. & Harris, N. C. Conceptualizing the 3D niche and vertical space use. *Trends Ecol. Evol.* **37**, 953–962 (2022).

33. Tokeshi, M. & Arakaki, S. Habitat complexity in aquatic systems: fractals and beyond. *Hydrobiologia* **685**, 27–47 (2012).

34. Klages, J. P. *et al.* Temperate rainforests near the South Pole during peak Cretaceous warmth. *Nature* **580**, 81–86 (2020).

35. Harris, P. T., Macmillan-Lawler, M., Rupp, J. & Baker, E. K. Geomorphology of the Oceans. *Mar. Geol.* **352**, 4–24 (2014).

36. Gray, M. *Geodiversity: Valuing and Conserving Abiotic Nature*. (Wiley-Blackwell, 2013).

37. Hjort, J. *et al.* Towards a taxonomy of geodiversity. *Philos. Trans. R. Soc. A* **382**, 1–14 (2024).

38. Tukiainen, H., Bailey, J. J., Field, R., Kangas, K. & Hjort, J. Combining geodiversity with climate and topography to account for threatened species richness. *Conserv. Biol.* **31**, 364–375 (2017).

39. Shi, T., Li, X., Xin, L. & Xu, X. The spatial distribution of farmland abandonment and its influential factors at the township level: A case study in the mountainous area of China. *Land Use Policy* **70**, 510–520 (2018).

40. Fahrig, L. *et al.* Functional landscape heterogeneity and animal biodiversity in agricultural landscapes. *Ecol. Lett.* **14**, 101–112 (2011).

41. Meehan, T. D., Werling, B. P., Landis, D. A. & Gratton, C. Agricultural landscape simplification and insecticide use in the Midwestern United States. *Proc. Natl. Acad. Sci.* **108**, 11500–11505 (2011).

42. Wang, T., Belle, I. & Hassler, U. Modelling of Singapore's topographic transformation based on DEMs. *Geomorphology* **231**, 367–375 (2015).

43. Valente, L. *et al.* A simple dynamic model explains the diversity of island birds worldwide. *Nature* **579**, 92–96 (2020).

44. Igea, J. & Tanentzap, A. J. Global topographic uplift has elevated speciation in mammals and birds over the last 3 million years. *Nat. Ecol. Evol.* **5**, 1530–1535 (2021).

45. Ellis, E. C. *et al.* People have shaped most of terrestrial nature for at least 12,000 years. *Proc. Natl. Acad. Sci.* **118**, e2023483118 (2021).

46. Sullivan, A. P., Bird, D. W. & Perry, G. H. Human behaviour as a long-term ecological driver of non-human evolution. *Nat. Ecol. Evol.* **1**, 1–11 (2017).

47. Flores, B. M. & Levis, C. Human-food feedback in tropical forests. *Science* **372**, 1146–1147 (2021).

48. R Core Team. R: A language and environment for statistical computing. R Foundation for Statistical Computing (2022).

49. QGIS.org. QGIS Geographic Information System. QGIS Association (2023).

50. Madin, J. & Schiettekatte, N. habtools: Tools and Metrics for 3D Surfaces and Objects. (2024).

51. Microsoft Corporation & Weston, S. doParallel: Foreach Parallel Adaptor for the ‘parallel’ Package. (2022).

52. Microsoft Corporation & Weston, S. foreach: Provides Foreach Looping Construct. (2022).

53. Smith, B. & Sandwell, D. Accuracy and resolution of shuttle radar topography mission data. *Geophys. Res. Lett.* **30**, (2003).

54. Keith, D. A., Ferrer-Paris, J. R., Nicholson, E. & Kingsford, R. T. Indicative distribution maps for Ecosystem Functional Groups - Level 3 of IUCN Global Ecosystem Typology. (2023) doi:10.5281/zenodo.10081251.

55. Copernicus Climate Change Service. Land cover classification gridded maps from 1992 to present derived from satellite observation. (2019).

56. Hijmans, R. J. raster: Geographic data analysis and modeling. (2020).

57. Bürkner, P. brms: An R Package for Bayesian Multilevel Models Using Stan. *J. Stat. Softw.* **80**, 1–28 (2017).

58. Polman, E. M. N., Seijmonsbergen, A. C., Versteegh, H. & Kissling, W. D. Global geodiversity components are not equally represented in UNESCO Global Geoparks. *Philos. Trans. R. Soc. A* **382**, 1–18 (2024).

59. Center for International Earth Science Information Network (CIESIN). Gridded Population of the World, Version 4 (GPWv4): Population Count, Revision 11. (2018).

60. Wood, S. N. *Generalized Additive Models*. (Chapman and Hall/CRC, New York, 2017). doi:10.1201/9781315370279.

61. Hijmans, R. J. terra: Spatial Data Analysis. (2023).

Figures & Tables

Figure 1. Global patterns in structural habitat complexity. High resolution maps (1.87 × 1.87 km) depicting patterns in the geometric complexity measures of **(a)** Fractal Dimension (*D*), **(b)** Rugosity (*R*), and **(c)** Height Range (*ΔH*), across all terrestrial and marine environments. Each map is displayed in a global Mollweide equal area projection and comprises ~146 million estimates of *ΔH*, *R*, and *D*, with white pixels reflecting missing or omitted entries.

Figure 2. The relative complexity characteristics of differing global environments offer insight into the differing structural regimes underlying different ecosystems. Comparisons of the fractal dimension (*D*) and rugosity (*R*, displayed following log10 transformation) patterns across the **(a)** Amazonian Basin, **(b)** Mariana Trench, and **(c)** Sahara Desert. Each map displays a 935 × 935 km section of selected locations and are displayed in a global Mollweide equal area projection, with latitude and longitude in metres. Inset photographs (obtained from www.freepik.com) offer a visualisation of how the landscapes associated with the Amazon Rainforest and the Sahara desert translate into their associated complexity regimes.

Figure 3. The rugosity and fractal dimension characteristics of natural environments situate differing ecosystem types along a complexity gradient and offer insight into the relationship between habitat structure and the anthropogenic use and change of local environments. (a) Ecosystems (categorised using the IUCN function-based ecosystem typology[11]) can be arranged along a complexity gradient based on their mean fractal dimension (*D*) and rugosity (*R*) characteristics. Solid line represents the predicted relationship between ecosystem estimates of *R* and *D*, with the shaded region identifying the 95% confidence intervals of these predictions. Dashed lines highlighting the position of selected ecosystem classifications. **(b)** Comparing the mean rugosity and fractal dimension characteristics of

differing land cover classifications. Land cover categories and their spatial distributions obtained from the Copernicus Climate Change Service (C3S) land cover survey[55]. Solid line represents the relationship between land use type estimates of *R* and *D* predicted using our Bayesian model parameterised using ecosystem type estimates of *R* and *D*. Dashed lines highlighting the three primary human modified land cover types within the C3S classification.

Figure 4. Evaluating the association of geological, climatic, and societal patterns with geometric habitat structure highlights mechanisms through which habitat complexity refines the global configuration of society and nature. The association between each of the structural complexity measures of Height Range (ΔH), Rugosity (R), and Fractal Dimension (D), and global **(a)** geodiversity, and **(b)** human population density. Geodiversity estimates were extracted from a high resolution (1.87 × 1.87 km) global map depicting patterns in the richness of structural features comprising an environment[58]. The solid line across each plot represents the predicted relationship between each geodiversity and each complexity measure, with the thickness of the line corresponding with the 95% confidence intervals. Human population density patterns were sourced from the Gridded Population of the World[59], with each plot showing the predicted relationships (including 95% CI) derived from two-part hurdle models separately exploring patterns in the probability of zero population densities (red) and population count densities (blue). Population density estimates were transformed using a power transformation ($y^{0.05}$).

Figure 1

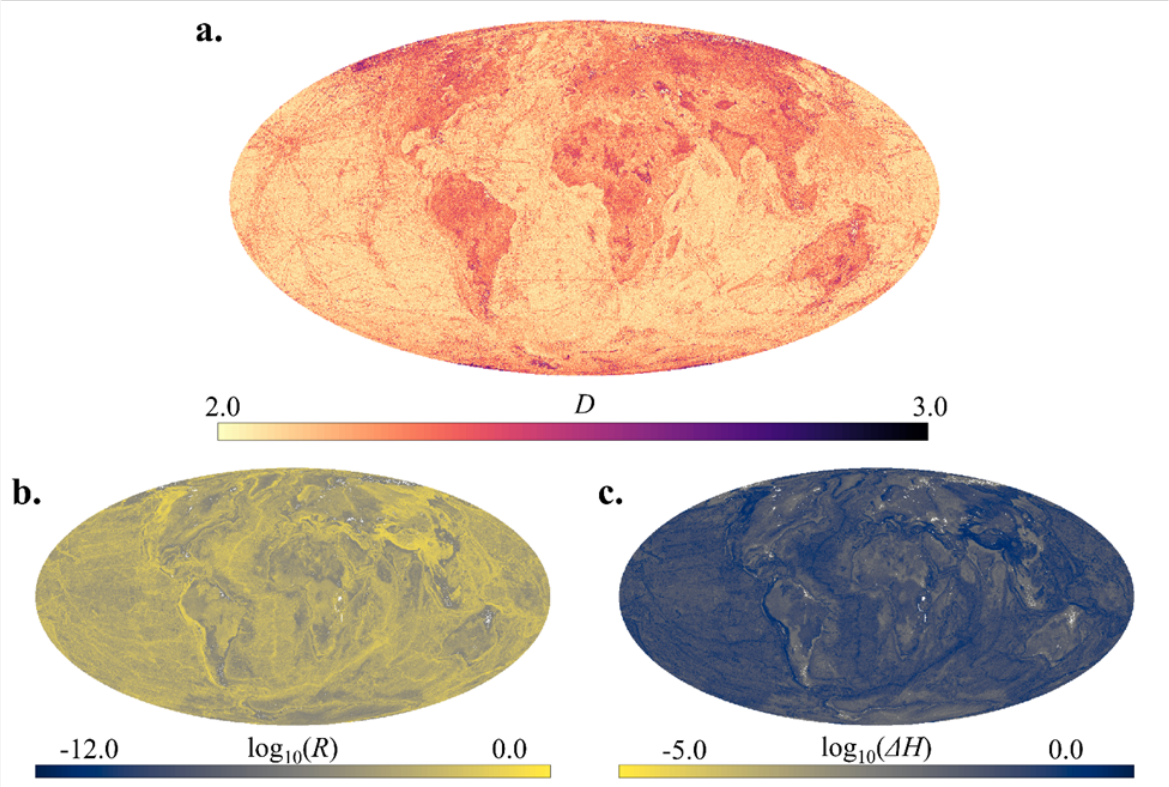

Figure 2

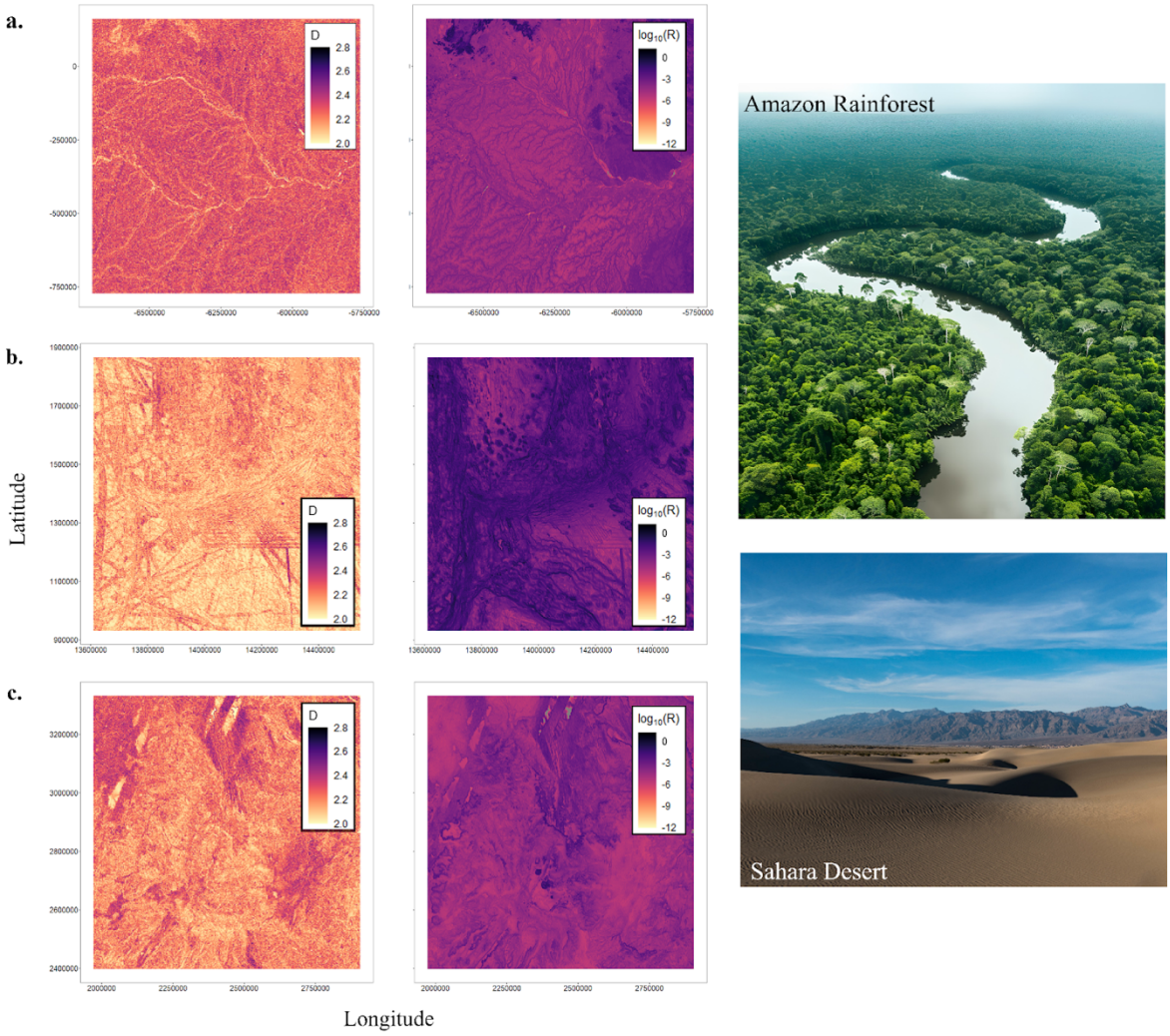
a.
b.
c.
D
2.8
2.6
2.4
2.2
2.0
log10(R)
0
-3
-6
-9
-12
Latitude
Longitude
Amazon Rainforest
Sahara Desert

548 **Figure 3**

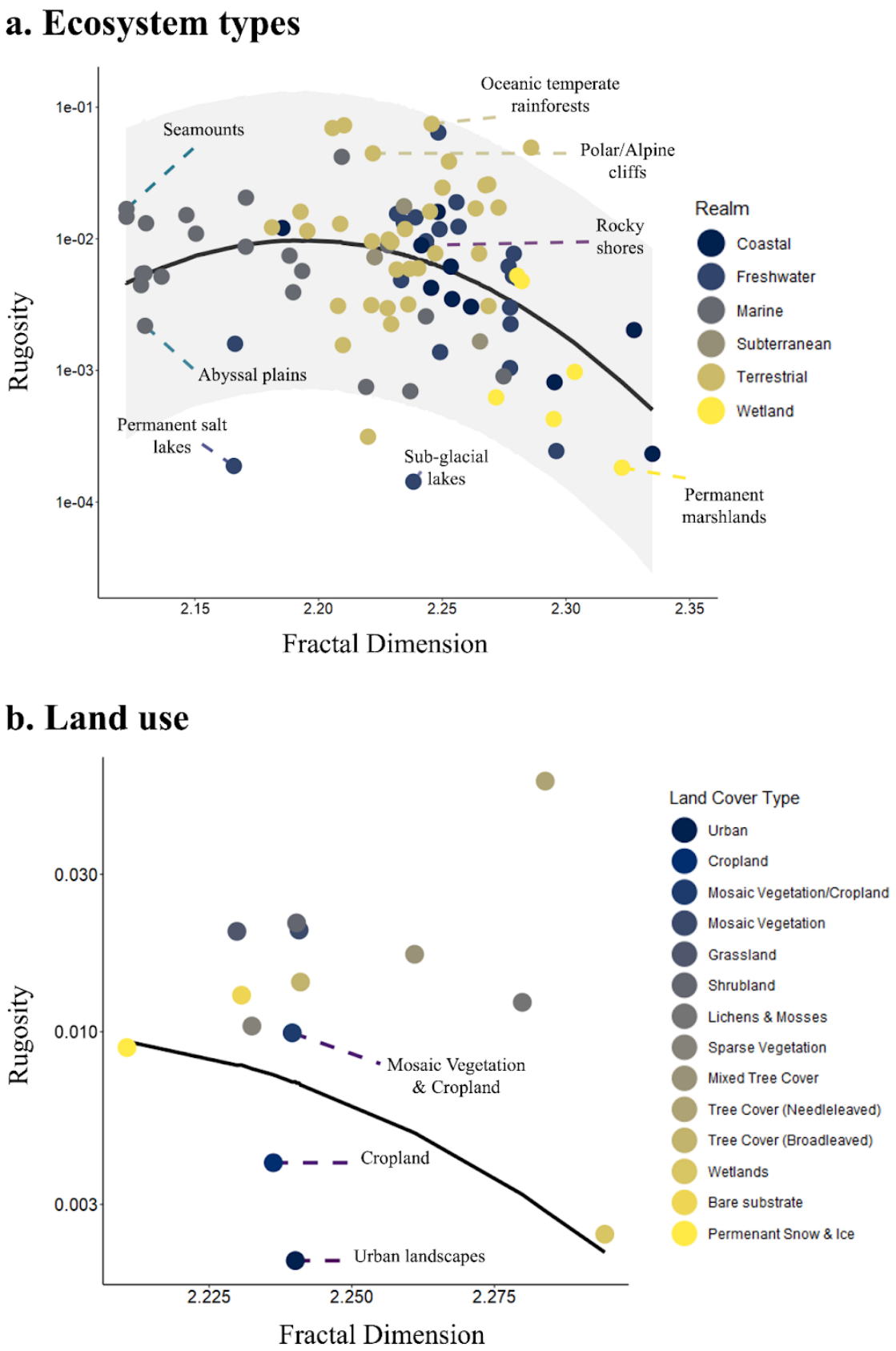
a. Ecosystem types
Oceanic temperate rainforests
Seamounts
Polar/Alpine cliffs
Rocky shores
Abyssal plains
Permanent salt lakes
Sub-glacial lakes
Permanent marshlands
Realm
Coastal
Freshwater
Marine
Subterranean
Terrestrial
Wetland
Rugosity
1e-01
1e-02
1e-03
1e-04
2.15
2.20
2.25
2.30
2.35
Fractal Dimension
b. Land use
Land Cover Type
Urban
Cropland
Mosaic Vegetation/Cropland
Mosaic Vegetation
Grassland
Shrubland
Lichens & Mosses
Sparse Vegetation
Mixed Tree Cover
Tree Cover (Needleleaved)
Tree Cover (Broadleaved)
Wetlands
Bare substrate
Permenant Snow & Ice
Mosaic Vegetation & Cropland
Cropland
Urban landscapes
Rugosity
0.030
0.010
0.003
2.225
2.250
2.275
Fractal Dimension

549 **Figure 4**

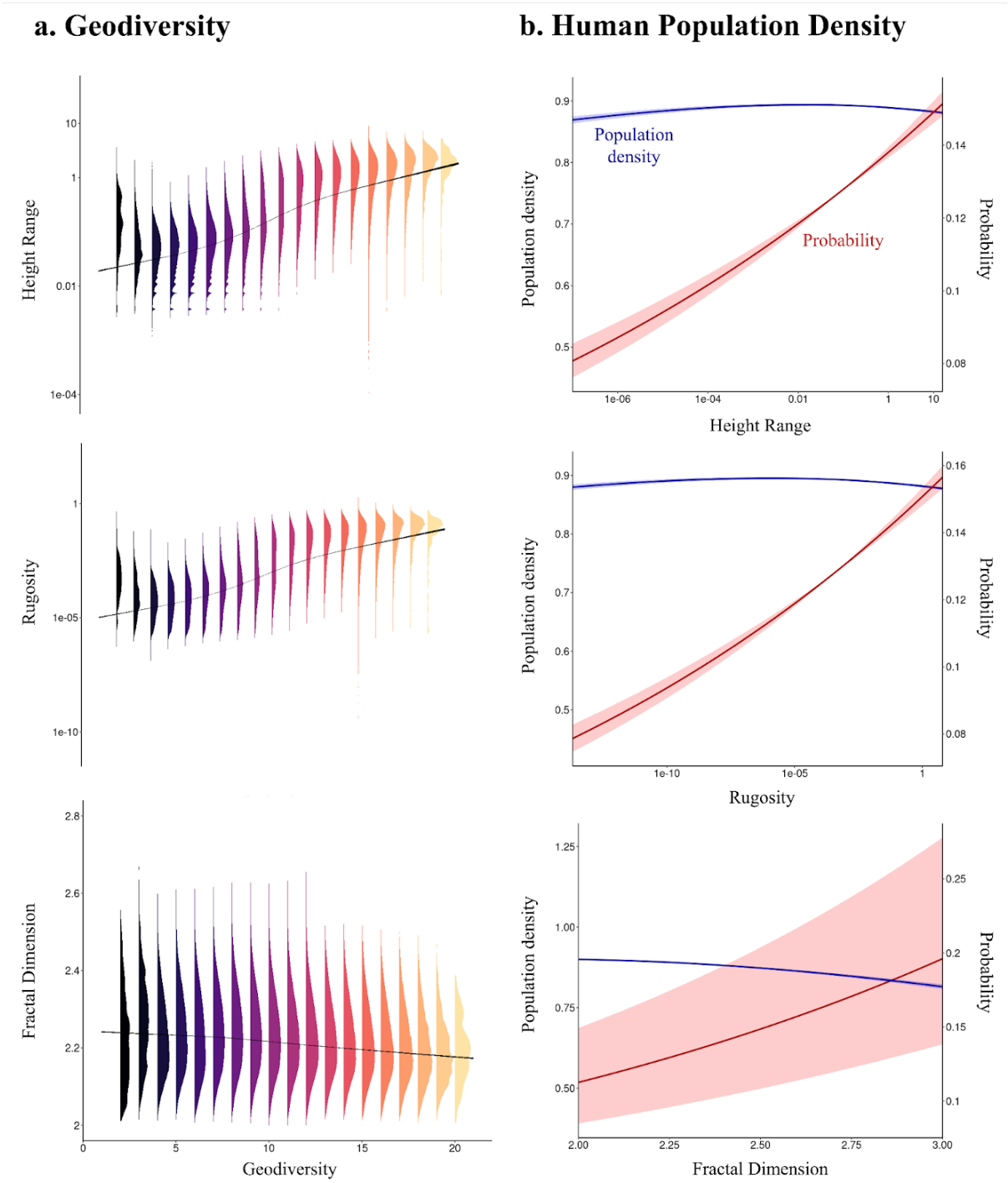

550

551
552